List of Supplemental Materials

Supplemental Figure S1. Single deletion of *SSA1, SSA2, SSA3* or *SSA4* does not stabilize Ndc10-2.

Supplemental Figure S2. A genetic screen for the identification of the Hsp40 co-chaperone required for Ndc10-2 degradation.

Supplemental Figure S3. The stabilization of Vma12-*DegAB* in *sis1-85* cells is independent of prion infection.

Supplemental Figure S4. Vma12-$DegAB_{\Delta 10}$ does not interact with Doa10.

Supplemental Figure S5. GFP-$DegAB_{\Delta 10}$ is not sequestered into QC foci in *ssa1/2Δ* cells.

Supplemental Figure S6. GFP-$DegAB_{DD}$ is soluble in *wild-type* cells but appears in punctate foci in *ssa1/2Δ* cells.

Supplemental Figure S7. Growth and FACS analysis of strains transformed with GFP-*DegAB.*

Supplemental Table S1. Degradation characteristics of Ndc10 and its degron derivatives used in this study.

Supplemental Table S2. Yeast strains used in this study.

Supplemental Table S3. Plasmids used in this study

Supplemental Video S1. GFP-*DegAB* foci display asymmetric inheritance in *ssa1/2Δ* cells. Time-dependent changes in the localization of GFP-*DegAB*. GFP-*DegAB* was visualized in the indicated strains by fluorescence microscopy. Images were collected from logarithmically growing cells at 5 min intervals. 5 frames/second display rate.

Supplemental Video S2. GFP-*DegAB* display diffused accumulation in *doa10Δ* cells. Time-dependent changes in the localization of GFP-*DegAB*. GFP-*DegAB* was visualized in the indicated strains by fluorescence microscopy. Images were collected from logarithmically growing cells at 5 min intervals. 5 frames/second display rate.

Figure S1. Single deletion of *SSA1*, *SSA2*, *SSA3* or *SSA4* does not stabilize Ndc10-2. The degradation of FLAG tagged ndc10-2 in the indicated strains was analyzed by CHX-chase followed by immunobloting.

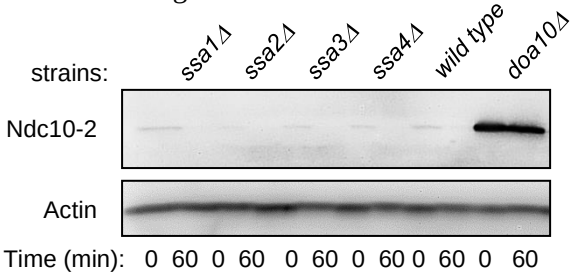

Figure S2. A genetic screen for the identification of the Hsp40 co-chaperone required for Ndc10-2 degradation. (A) A screen for Non-essential J proteins involved in PQCD: Steady-state levels of Ndc10-2 were measured in yeast knockout strains lacking genes encoding various J proteins. Mdj1 and Jid1 J proteins, which are localized to the inner mitochondrial matrix, served as negative controls. (B and C) A screen for essential J proteins involved in PQCD: Ndc10-2 levels in the indicated strains were assayed by cycloheximide chase and immunoblotting. (B) The contribution of Caj1 to Ndc10-2 stability was analyzed in *Caj1 Tet off* cells where Caj1 is expressed from a tetracycline titratable promoter. *Pre6-Tet off* cells where the α4 subunit of the proteasome Pre6 is expressed under the same promoter served as control. (C) Cwc23, involvement in Ndc10-2 degradation was analyzed in *cwc23Δ* strains harboring either *Cwc23* wild type allele or *cwc23 ΔJ* mutant (Δ2-80aa) on a plasmid. *Asterisk* (*) indicates a Flag antibody nonspecific band that was used as loading control.

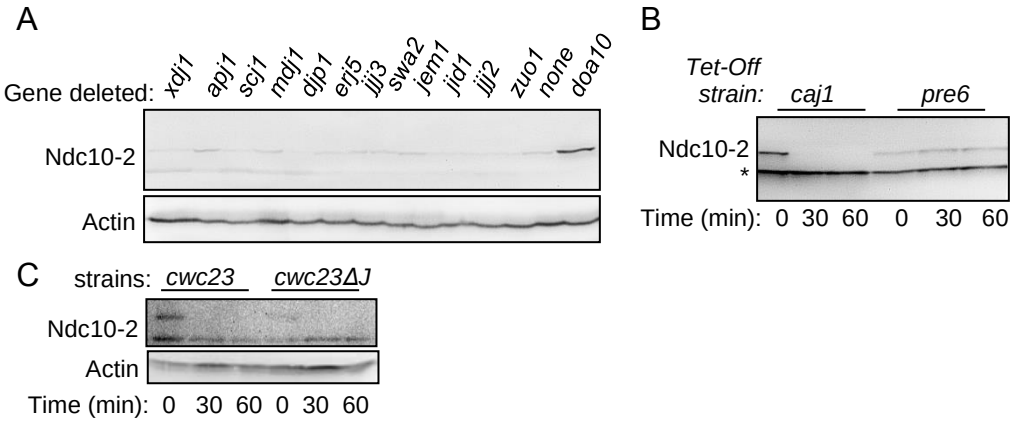

Figure S3. The stabilization of Vma12-*DegAB* in *sis1-85* cells is independent of prion infection.

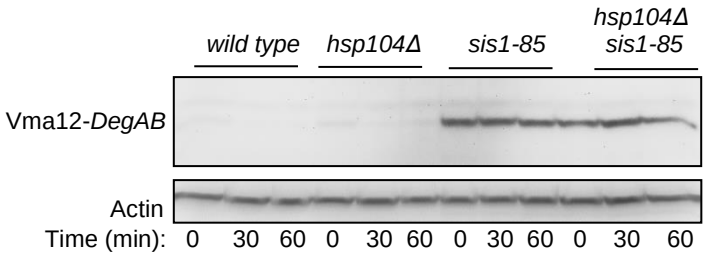

Figure S4. Vma12-*DegAB*$_{\Delta 10}$ does not interact with Doa10**.** Doa10-13myc was immunoprecipitated from digitonin-solubilized microsomes with anti Myc antibodies. Substrate co-imunoprecipitation was analyzed by immunoblotting with anti-FLAG antibodies.

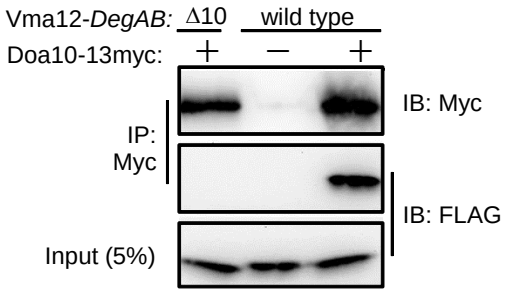

Figure S5. GFP-*DegAB*$_{\Delta 10}$ is not sequestered into QC foci in *ssa1/2Δ* cells. *Green channel: GFP; Red channel: Hoechst*. The scale bar represents 5 µm.

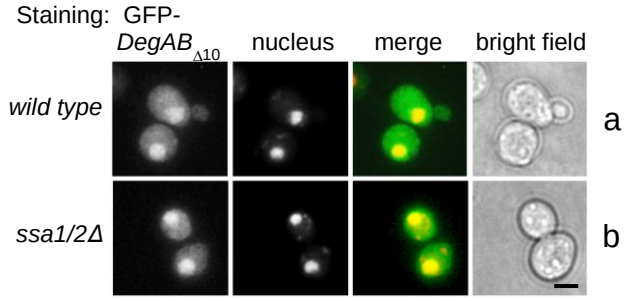

Figure S6. GFP-*DegAB*$_{DD}$ is soluble in *wild-type* cells but appears in punctate foci in *ssa1/2Δ* cells. *Green channel: GFP; Red channel: Hoechst*. The scale bar represents 5 µm.

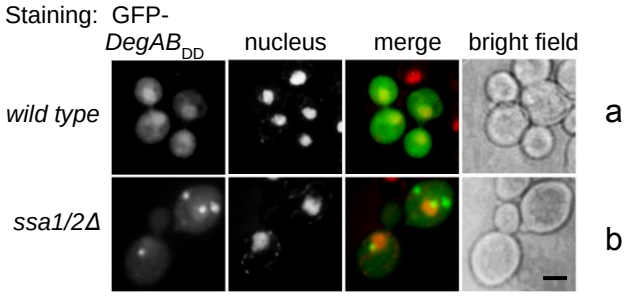

Figure S7. Growth and flow cytometry analysis of strains transformed with GFP-*DegAB*. (A) The indicated strains were grown to the same density, then spotted as 5 fold serial dilution onto SD-Trp agar plates and incubated at 30°C or 37°C for 2 days. (B) Cell fluorescence levels during logarithmic growth were assessed by flow cytometry. GFP-positive cells were identified using 2-dimensional dot plots of red (PE) versus green (GFP) fluorescence. GFP-positive cells were enriched by FACS (2 – 10 x 10^4 cells were collected) using the diagonal gate indicated in the plots, and returned to culture conditions. Flow cytometry analysis of the cells before and after sorting is shown in the top and bottom graphs respectively and was used to calculate the relative percentages of GFP-positive and -negative cells (shown in C).

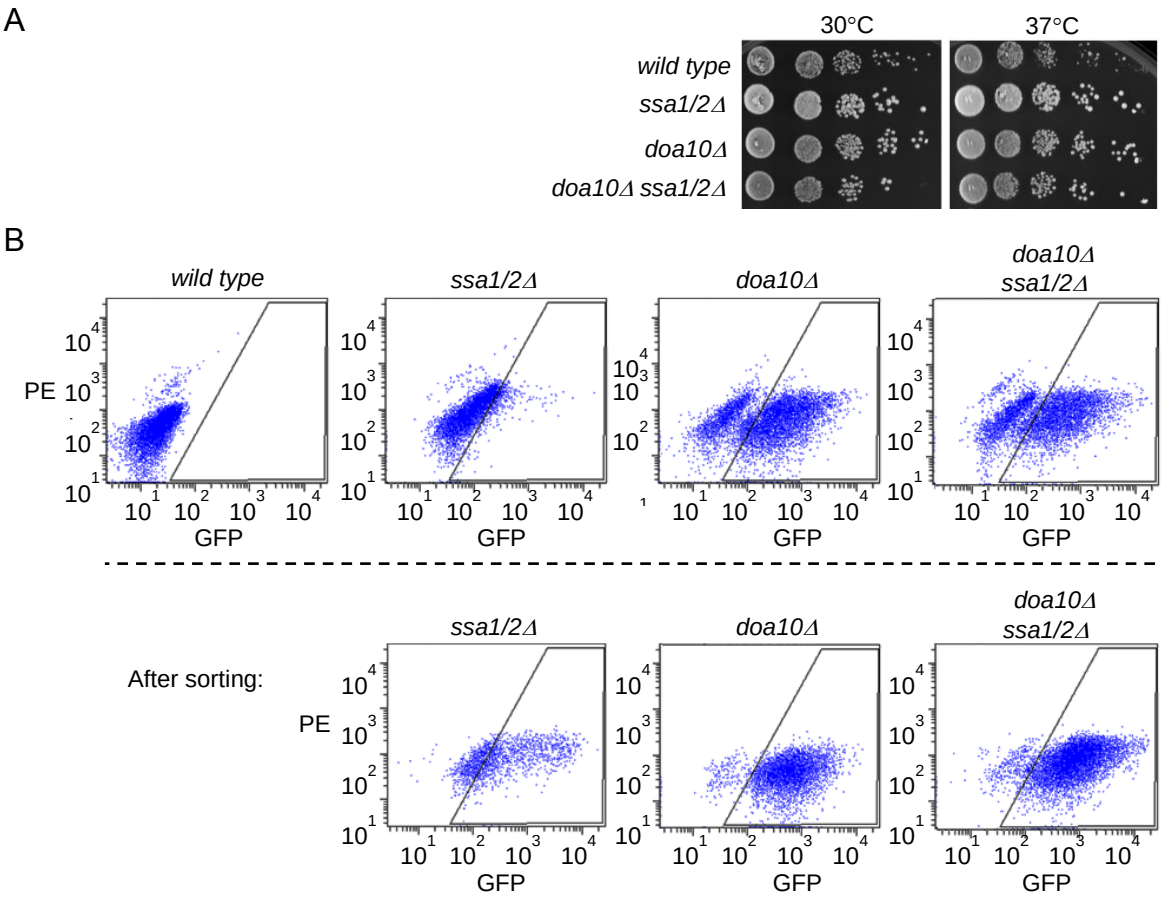

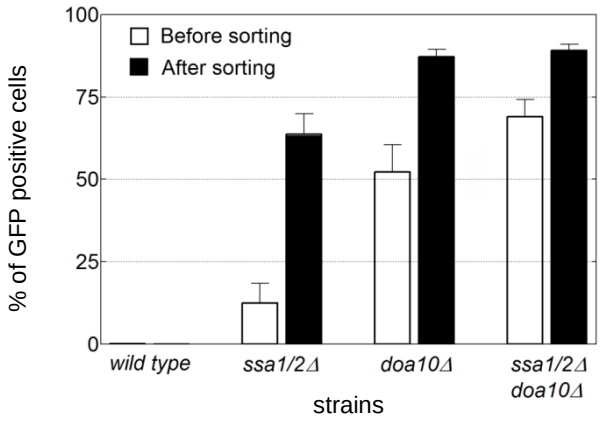

Supplemental Tables

Table S1. Degradation characteristics of Ndc10 and its degron derivatives used in this study.

Substrate	Stability	Ubiquitylation	localization	E3	Hsp70/40 involved
Ndc10-2	–	+	Nucleus (Punctate)	Doa10	Ssa1/2, Sis1 (weak)
Vma12-*DegAB*	–	+	ER		Ssa1/2, Sis1
Vma12-*DegAB* $_{DD}$	+	+	ER		
Vma12-GFP-*DegAB*	–	+	ER		
GFP-*DegAB*	–	+	Nucleus (Diffused)		
GFP-*DegAB*$_{DD}$	+	+	Nucleus (Diffused)		
GFP-*DegAB*$_{\Delta 10}$	+	–	Nucleus (Diffused)	N/A	N/A
Vma12-*DegAB*$_{\Delta 10}$	+	–	ER	N/A	N/A

N/A – not applicable

These annotations are based on findings emerged from our previous studies (Furth *et al*., 2012, Alfassy *et al*., 2013) as well the current study.

Table S2: Yeast strains used in this study.

Yeast	**Genotype**	**Source**
TRY123	*α his3-11,15, leu2-3,112, ura3-52, trp1-1, ade2-1, can 1-100, lys2Δ*	(Sanchez *et al.*, 1993)
TRY124	*a ade2-1, his3-11,15, leu2-3,112, ura3-1, trp1-1, ssdl-d2, can1-100, lys2Δ hsp104::URA3*	(Sanchez *et al.*, 1993)
TRY125	*α his3-11,15, leu2-3,112, ura3-52, trp1-1, ade2-1, can 1-100, lys2Δ, ssa1::HIS3, ssa2::LEU2*	(Sanchez *et al.*, 1993)
TRY169	*α his3-11,15, leu2-3,112, ura3-52, trp1-1, ade2-1, can 1-100, doa10-Δ1::HIS3*	M. Hochstrasser
TRY334	*α his3-11,15, leu2-3,112, ura3-52, trp1-Δ1, lys2, SSA1, ssa2::LEU2, ssa3::TRP1, ssa4::LYS2*	(Becker *et al.*, 1996)
TRY335	*α his3-11,15, leu2-3,112, ura3-52, trp1-Δ1, lys2, ssa1ts (ssa1-45), ssa2-1::LEU2, ssa3-1::TRP1, ssa4-2::LYS2*	(Becker *et al.*, 1996)
TRY 581	*α ade2-1, his3-11, leu2-3112, ura3-1, trp1-1, can 1-100*	(Thomas and Rothstein, 1989)
TRY582	*α ade2-1, his3-11, leu2-3112, ura3-1, trp1-1, can 1-100, ydj1-2::HIS3, LEU2::ydj1-151*	(Caplan *et al.*, 1992)
TRY583	*a ade2-1, his3-11,15, leu2-3112, ura3-1, trp1-1, ssdl-d2, can1-100, sis1::HIS3, SIS1* on *CEN/LEU2* plasmid	(Luke *et al.*, 1991)

Yeast	Genotype	Source
TRY584	*a ade2-1, his3-11,15, leu2-3112, ura3-1, trp1-1, ssdl-d2, can1-100, sis1::HIS3, NH2–HA*-tagged *sis1-85* on*CEN/LEU2* plasmid	(Luke *et al.*, 1991)
TRY1259	a *his3Δ1, leu2Δ0, met15Δ0, ura3Δ0:: URA::CMV-tTA, Kan-tetO7-CAJ1*	(Hughes *et al.*, 2000)
TRY879	a *his3Δ1, leu2Δ0, met15Δ0, ura3Δ0:: URA::CMV-tTA, Kan-tetO7-PRE6*	(Hughes *et al.*, 2000)
TRY1113	*ade2-1, his3-11,15, leu2-3,112, ura3-1, trp1-1, ssdl-d2, can1-100, lys2-2 cwc23::KanMX, CWC23* on *CEN/URA1* plasmid	(Sahi *et al.*, 2010)
TRY1114	*ade2-1, his3-11,15, leu2-3,112, ura3-1, trp1-1, ssdl-d2, can1-100, lys2-2 cwc23::KanMx, CWC23ΔJ* on *CEN/TRP1* plasmid	(Sahi *et al.*, 2010)
TRY1120	*α his3-11,15, leu2-3,112, ura3-52, trp1-1, ade2-1, can 1-100, lys2Δ, ssa1::HIS3, ssa2::LEU2, doa10::KanMX*	This study
TRY1208	*a ade2-1, his3-11,15, leu2-3112, ura3-1, trp1-1, ssdl-d2, can1-100, hsp104::URA3, sis1::HIS3, SIS1* on *CEN/LEU2* plasmid	This study
TRY1212	*a ade2-1, his3-11,15, leu2-3112, ura3-1, trp1-1, ssdl-d2, can1-100, hsp104::URA3, sis1::HIS3, NH2–HA*-tagged *sis1-85* on*CEN/LEU2* plasmid	This study
TRY1259	a *his3Δ1, leu2Δ0, met15Δ0, ura3Δ0:: URA::CMV-tTA, Kan-tetO7-CAJ1*	(Hughes *et al.*, 2000)
TRY1270	*α his3-11,15, leu2-3,112, ura3-52, trp1-1, ade2-1, can 1-100, lys2Δ, ssa1::HIS3, ssa2::LEU2, hsp42::KanMX*	This study

Table S3: Plasmids used in this study.

Plasmid	Relevant markers	Source
pTR338	pET11a-Ubc6$_{225aa}$-His$_6$	This study
pTR851	pRS415GPD$_p$-Δ11Ndc10-FLAG-Cyc1$_t$	(Furth *et al.*, 2011)
pTR852	pRS415GPD$_p$-Δ11ndc10-2-FLAG-Cyc1$_t$	(Furth *et al.*, 2011)

Plasmid	Relevant markers	Source
pTR875	pRS414GPD$_p$- FLAG-Vma12-GFP-*DegAB*-Cyc1$_t$	This study
pTR828	pRS410GPD$_p$- FLAG-Vma12-6HIS- *DegAB*-Cyc1$_t$	(Furth *et al.*, 2011)
pTR913	pRS414GPD$_p$- FLAG-Vma12-6HIS- *DegAB*-Cyc1$_t$	This study
pTR937	pRS414GPD$_p$-GFP-*DegAB*-Cyc1$_t$	This study
pTR941	pCPY*-HA *(CEN/TRP1)*	(Ng *et al.*, 2000)
pTR949	pRS416GPD$_p$- Δ11Ndc10-2-FLAG-Cyc1$_t$	(Furth *et al.*, 2011)
pTR990	pCUP1$_p$ -Ubiquitin *(CEN/LYS2)*	M. Hochstrasser
pTR1114	pRS414 GPD$_p$- FLAG-Vma12-6HIS - *DegAB*$_{L950D,L951D}$-Cyc1$_t$	(Furth *et al.*, 2011)
pTR1163	pRS316- GPD$_p$-Hsp42-Cherry	(Kaganovich *et al.*, 2008)
pTR1245	pRS416 TEF$_p$-6HIS-*SSA1*- Cyc1$_t$	(Pfund *et al.*, 2001)
pTR1380	pRS414GPD$_p$- FLAG-Vma12-GFP-*DegAB*$_{Δ10}$-Cyc1$_t$	This study
pTR1378	pRS414GPD$_p$-GFP-*DegAB*$_{Δ10}$-Cyc1$_t$	This study
pTR1387	pRS414GPD$_p$-Δ11Ndc10-2-FLAG-Cyc1$_t$	This study
pTR1399	pRS414GPD$_p$-GFP-*DegAB* $_{L950D,L951D}$ -Cyc1t	This study

References for strains and plasmids

Becker, J., Walter, W., Yan, W., and Craig, E.A. (1996). Functional interaction of cytosolic hsp70 and a DnaJ-related protein, Ydj1p, in protein translocation in vivo. Mol Cell Biol *16*, 4378-4386.

Caplan, A.J., Cyr, D.M., and Douglas, M.G. (1992). YDJ1p facilitates polypeptide translocation across different intracellular membranes by a conserved mechanism. Cell *71*, 1143-1155.

Furth, N., Gertman, O., Shiber, A., Alfassy, O.S., Cohen, I., Rosenberg, M.M., Doron, N.K., Friedler, A., and Ravid, T. (2011). Exposure of bipartite hydrophobic signal triggers nuclear quality control of Ndc10 at the endoplasmic reticulum/nuclear envelope. Molecular Biology of the Cell *22*, 4726-4739.

Hughes, T.R., Marton, M.J., Jones, A.R., Roberts, C.J., Stoughton, R., Armour, C.D., Bennett, H.A., Coffey, E., Dai, H., He, Y.D., Kidd, M.J., King, A.M., Meyer, M.R., Slade, D., Lum, P.Y., Stepaniants, S.B., Shoemaker, D.D., Gachotte, D., Chakraburtty, K., Simon, J., Bard, M., and Friend, S.H. (2000). Functional discovery via a compendium of expression profiles. Cell *102*, 109-126.

Kaganovich, D., Kopito, R., and Frydman, J. (2008). Misfolded proteins partition between two distinct quality control compartments. Nature *454*, 1088-1095.

Luke, M.M., Sutton, A., and Arndt, K.T. (1991). Characterization of SIS1, a Saccharomyces cerevisiae homologue of bacterial dnaJ proteins. The Journal of cell biology *114*, 623-638.

Ng, D.T., Spear, E.D., and Walter, P. (2000). The unfolded protein response regulates multiple aspects of secretory and membrane protein biogenesis and endoplasmic reticulum quality control. The Journal of cell biology *150*, 77-88.

Pfund, C., Huang, P., Lopez-Hoyo, N., and Craig, E.A. (2001). Divergent functional properties of the ribosome-associated molecular chaperone Ssb compared with other Hsp70s. Mol Biol Cell *12*, 3773-3782.

Sahi, C., Lee, T., Inada, M., Pleiss, J.A., and Craig, E.A. (2010). Cwc23, an essential J protein critical for pre-mRNA splicing with a dispensable J domain. Mol Cell Biol *30*, 33-42.

Sanchez, Y., Parsell, D.A., Taulien, J., Vogel, J.L., Craig, E.A., and Lindquist, S. (1993). Genetic evidence for a functional relationship between Hsp104 and Hsp70. J Bacteriol *175*, 6484-6491.

Thomas, B.J., and Rothstein, R. (1989). The genetic control of direct-repeat recombination in Saccharomyces: the effect of rad52 and rad1 on mitotic recombination at GAL10, a transcriptionally regulated gene. Genetics *123*, 725-738.